

SHORT-FATIGUE-CRACK GROWTH-RATE MODELING BASED ON THE J-INTEGRAL AS THE CONTROLLING PARAMETER

MODELIRANJE HITROSTI RASTI KRATKE UTRUJENOSTNE RAZPOKE NA OSNOVI J-INTEGRALA KOT KONTROLNEGA PARAMETRA

Kun Fang¹, Pei Chen^{*}, Xinyao Zhang, Xiaoqin Zha, Yuhao Gao, Xianfu Luo

¹Luoyang Ship Material Research Institute, Luoyang 471023, P.R. China
²State Key Laboratory for Marine Corrosion and Protection, Luoyang 471023, P.R. China

Prejem rokopisa – received: 2024-02-26; sprejem za objavo – accepted for publication: 2024-08-26

doi:10.17222/mit.2024.1117

The local plasticity around the short fatigue crack tip fails to satisfy the basic assumption of linear-elastic fracture mechanics, which will lead to strong nonlinearity between da/dN and stress field strength indicator. Therefore, the elastic-plastic fracture mechanics parameter J -integral is employed to consider the non-uniform stress field. To this end, the *in-situ* observation system is set up to monitor and measure the short fatigue growth behavior in real time. The indicator ΔJ is analyzed based on recorded three-dimensional geometric parameters of the crack. The quantitative relationship is established to model the short fatigue crack's growth rate.

Keywords: short fatigue crack's growth rate, J -integral, *in-situ* observation, corrosion pit

Lokalna plastičnost okoli kratke utrujenostne razpoke ne zadovoljuje temeljne predpostavke modela linearno-elastične mehanike loma. To vodi do močne nelinearnosti med da/dN in indikatorjem trdnosti napetostnega polja. Zato, da so lahko upoštevali nehomogeno napetostno polje so uvedli J -integral kot lomno mehanski parameter. Avtorji tega članka so postavili sistem za *in-situ* opazovanje hitrosti rasti kratke utrujenostne razpoke v realnem času. Indikator ΔJ so analizirali na osnovi zabeleženih tri dimenzionalnih geometričnih parametrov razpoke in nato izdelali model za kvantitativni izračun hitrosti rasti kratke utrujenostne razpoke.

Ključne besede: hitrost rasti kratke utrujenostne razpoke, J -integral, *in-situ* opazovanje, korozijska jamica

1 INTRODUCTION

A fatigue crack's growth behaviour is crucial for the design of materials and engineering structures, mainly obtained according to standard tests (such as ASTM E647). Research shows that the fatigue-crack propagation in steel structures (e.g., a CNG cylinder) are closely related to the inherent defects of the material and localized corrosion.¹⁻⁶ The empirical formula employs the linear elastic stress-field intensity range ΔK as the controlling parameter, which was first proposed by Paris and Erdogan,⁷ as follows:

$$da/dN = C(\Delta K)^m \quad (1)$$

where ΔK is the stress-intensity factor, and C and m denote the material constants, respectively.

However, literature⁸ indicates that 90 % of the entire fatigue life is consumed by initiation and short crack growth. The material of 35CrMo steel used for a CNG cylinder is sensitive to the short-fatigue-crack propagation effect in the corrosive environment, resulting in a crack growth rate of the same order of magnitude as the long fatigue crack.⁹ It is dangerous in engineering appli-

cations to overestimate the service lifetime of materials by ignoring the short-fatigue-crack growth behaviours.¹⁰

The physically SFCG occurs immediately after the fatigue crack's initiation. The difference between long and short fatigue crack can be reflected in the fatigue crack's growth rate.¹¹

The long fatigue crack's growth (LFCG) rate is faster than that of the SFCG, which appears at the low ΔK region. The length of the short fatigue crack usually lies in the range of 0.5–2.0 mm. Due to the limitation of the geometric dimensions of the short fatigue crack, it is not feasible to measure the short fatigue crack's length indirectly (such as compliance method) during the SFCG test. In addition, the fatigue crack initiates and grows, accompanied by a certain range of yielding around the crack tip in the high strength and toughness metal materials, which leads to an inaccurate stress-field-intensity characterization and a biased evaluation of the SFCG behaviours. The paper measures the geometric parameter of the fatigue crack (Type I) based on *in-situ* observation and calculates the controlling parameter J , representing the stress field with a certain region of yielding, as shown in equation (2). The mathematical relationship is proposed to model the SFCG rate.

*Corresponding author's e-mail:
chenpei_lsmri@outlook.com (Pei Chen)

Table 1: Chemical composition of 35CrMo steel (w/%)

C	Si	Mn	P	S	P+S	Cr	Mo	Ni	Cu	Fe
0.32≈0.40	0.17≈0.37	0.40≈0.70	≤0.020	≤0.010	≤0.025	0.80≈1.10	0.15≈0.25	≤0.30	≤0.20	Bal.

Table 2: Mechanical behaviour of 35CrMo steel

Tensile stress σ_u (MPa)	Yield stress σ_y (MPa)	Elastic modulus E (GPa)	Elongation A (%)	Reduction of area Z (%)	Plane-strain fracture toughness K_{IC} (MPam ^{0.5})
698	520	206	25.5	74	202

$$J = \int_{\Gamma} W dy - p_{\alpha} \frac{\partial u_{\alpha}}{\partial x} ds \quad (2)$$

where W is the strain energy density, p and u indicate the stress and displacement component, respectively.

2 EXPERIMENTAL PART

2.1 Materials and specimen preparation

The tested material is 35CrMo steel, which is extensively consumed in the manufacture of pressure vessels. The chemical composition and mechanical behaviour of the material are shown in **Tables 1** and **2**.

In the high-cycle fatigue test, the plate specimen with an artificial corrosion pit is employed to conduct the test, as shown in **Figure 1**. The specimens are polished using an electrochemical method. The artificial corrosion pit is prepared as follows: (1) Using the drill bit with a diameter of 3 mm to make a pit of approximately 1 mm. (2) Covering and sealing the area outside the pit with paraffin and placing the specimen in the electrolyte (5000 mL pure water + 250 mL HCl + 500g NaCl) for pitting corrosion. (3) Using a constant voltage of 15 V for the elec-

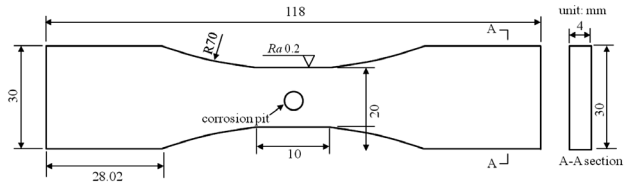


Figure 1: Plate specimen with artificial corrosion pit for SFCG test

trolyte, the corrosion pit's depth can reach the target value by controlling the total electrolysis time. In this paper, the corrosion pit parameter h/b is determined as 0.375 (i.e., $a = b = 4$ mm, $h = 1.5$ mm) to ensure that the short fatigue crack's initiation position and growth path can be tracked.

2.2. SFCG rate test

The specimens are fatigued using 100 kN MTS Landmark servo-hydraulic fatigue loading system (Model: MTS 810) equipped with high-resolution microscope (Model: VHX-600E), as shown in **Figure 2**. The fatigue loading is set as 26–520 MPa of the maximum stress during the test because the working-pressure range of the

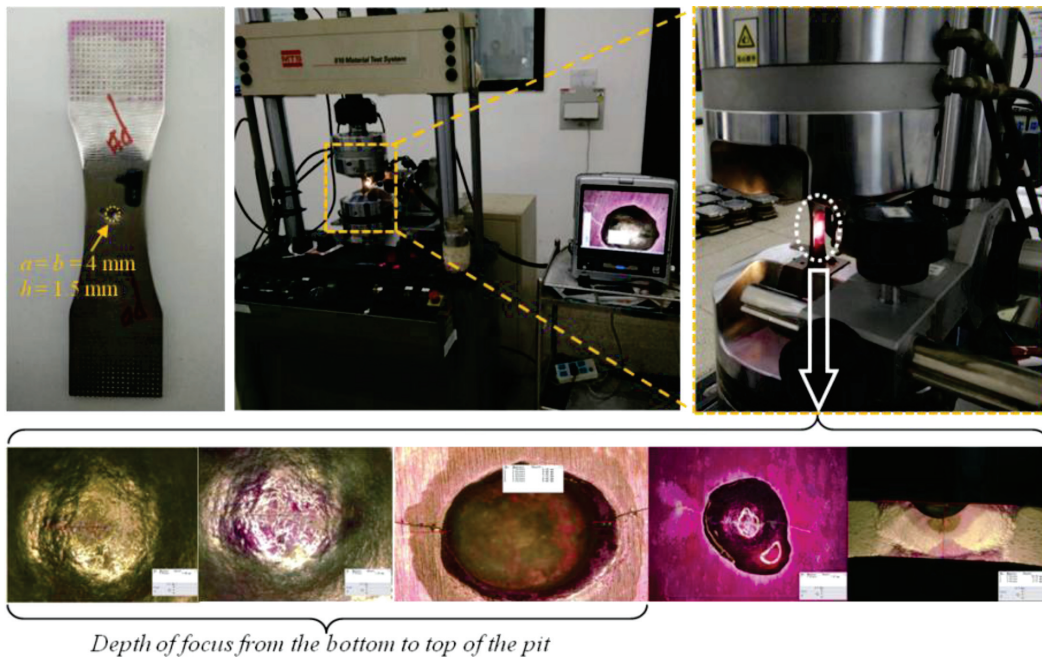


Figure 2: Short fatigue crack's characterization based on *in-situ* observation

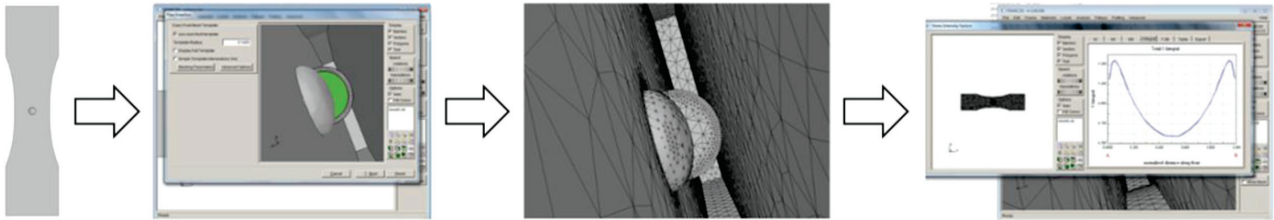


Figure 3: Calculation procedure of J -integral based on M-integral method

vessels is usually 5–100 % of the specified value. The fatigue loading frequency is set to 1 Hz. After the fatigue crack's initiation, the fatigue loading frequency is reduced as 0.25 Hz to ensure that the SFCG data is recorded stably.

To measure the short fatigue crack's length along the specimen thickness for a specific fatigue cycle, the penetration colouring method is employed to record the planar morphology of the short fatigue crack's tip.

The use of *in-situ* observation has achieved the purpose of measuring the length of small physical cracks. **Figure 2** depicts the short fatigue crack's length observation and measurement procedure.

Meanwhile, the fatigue loading cycle interval between two contiguous observations is also gradually reduced to ensure that the SFCG length recorded each time is between 100 μm and 300 μm .

Based on the penetration colouring method, 5–6 points at the fatigue crack's front edge are recorded for polynomial fitting of the relationship of the fatigue crack length $2c$ and depth h along the width and thickness of the test specimen. Thus, the SFCG length can be determined according to the surface fatigue crack length $2c$.

3 RESULTS AND DISCUSSION

3.1. Short fatigue crack front stress field characterization

The growth behaviour of a short fatigue crack is quite different from that of a long fatigue crack. At the SFCG stage, the crack-tip plastic zone fails to meet the assumption of the linear elastic fracture mechanics. Thus, the nonlinear elastic-plastic fracture mechanics parameters are considered as the driving force indicator that describes the SFCG behaviour. In the paper, the fatigue crack-tip field is characterized by the J -integral. The value of the J -integral is calculated based on the observed fatigue-crack length as follows: (1) The specimen is modelled, meshed and constrained based on ABAQUS software. The meshed and constrained model is stored in an .inp file. (2) Importing the .inp file into the Franc 3D software and adding a semi-elliptical crack surface in the bottom of the corrosion pit, the reconstructed model is meshed by considering the fatigue crack's surface. (3) The stress field is analysed in the statistical analysis module of the Franc3D software, calling the ABAQUS software solver. (4) The crack-tip energy field J -integral along the longitudinal and radial direction of the crack

tip is calculated based on the M-integral method.¹² The calculation procedure is shown in **Figure 3**.

The ΔK versus da/dN curves are still widely used in current literature, even though it is limited to the linear-elastic condition around the fatigue crack's tip. Thus, the empirical formula is employed to calculate the J -integral based on ΔK according to ASTM E1820-24, shown as follows:

$$\Delta K = \sqrt{\frac{E\Delta J}{1-\nu^2}} \quad (3)$$

where E is the elastic modulus and ν denotes the Poisson's ratio.

3.2. SFCG rate modeling

The curves of the fatigue crack's growth rate versus ΔJ of the four plate specimens with artificial corrosion pit are shown in **Figure 4**. The fatigue crack's growth data represents two stages with dramatic differences in the growth rate. The parameter ΔJ at the separator line lies in 5–9 kJ/m^2 . Meanwhile, the fatigue crack's length recorded by the *in-situ* observation is in the range 3.59–3.83 mm. The fatigue crack's growth data in the low ΔJ stage, i.e., the data in black solid rectangle, shows regular fluctuation, which is considered as the SFCG behaviours. The fatigue crack that grows stably at a certain growth rate with a high ΔJ value, i.e., the data in dashed ellipse, conforms to the long-crack growth behaviour in the famous Paris empirical formula. Besides, **Figure 4** indicates that the short and LFCG rates are equivalent at the initial stage of the long crack's growth, which means that the SFCG behaviour is critical in the safety evaluation of LNG cylinders. The SFCG rate can be fitted with the following three-order polynomial as follows:

$$da/dN = A_0 + A_1(\Delta J) + A_2(\Delta J)^2 + A_3(\Delta J)^3 \quad (4)$$

For the 35CrMo steel, the SFCG rate is in the range of $(0.3\text{--}1.5)\times 10^{-3}$ mm/cycle. The SFCG rate increases with the stress field indicator ΔJ first and then decreases. The conversion value of the SFCG rate is in the range of 3.7–6.2 kJ/m^2 . The low-order coefficients have a larger value, which means that there is a good linear relationship between the SFCG rate and the proposed controlling parameter ΔJ . Due to the existence of the conversion value of the SFCG rate, there is a strong nonlinear char-

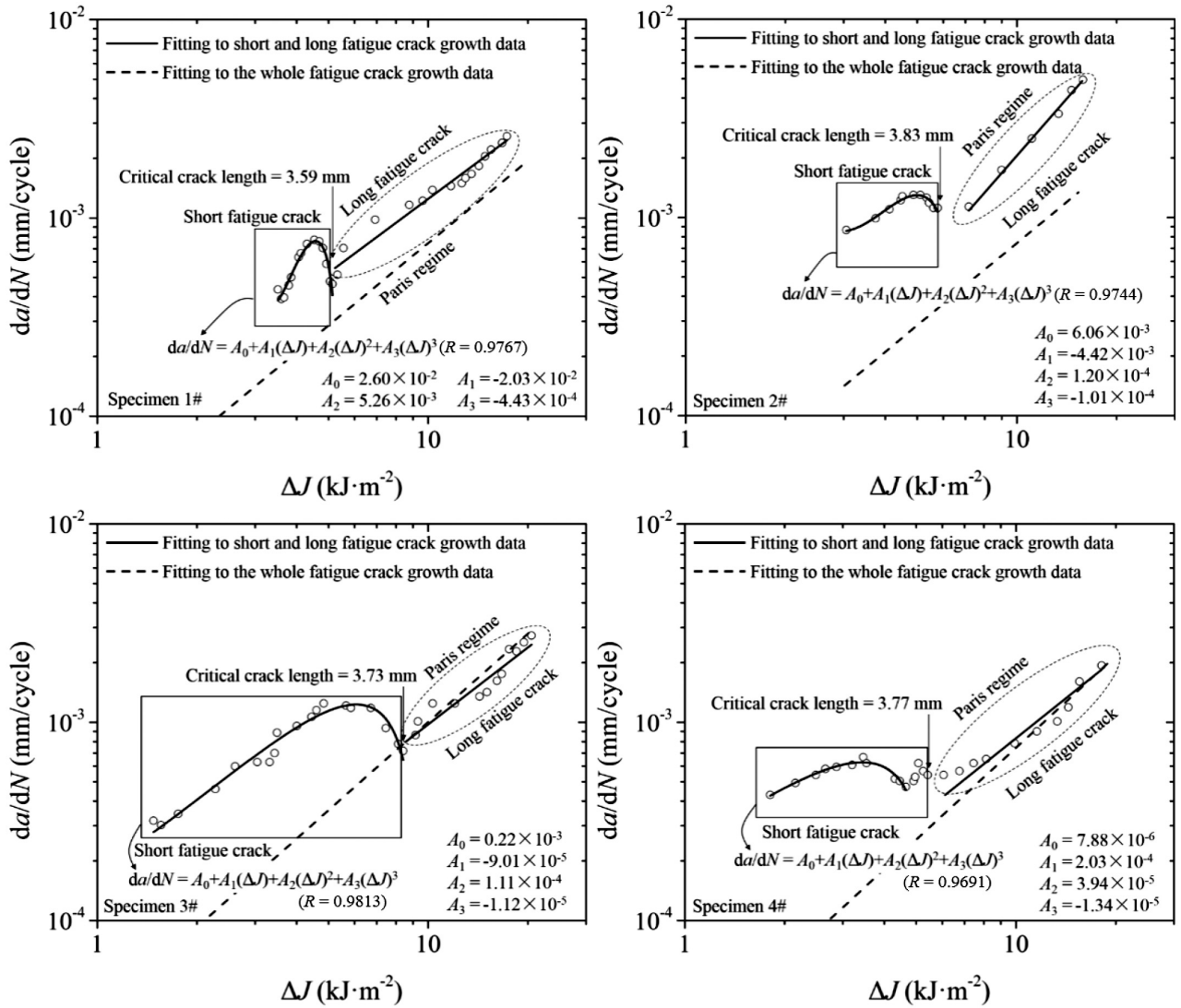


Figure 4: Curves of fatigue-crack growth rate versus ΔJ

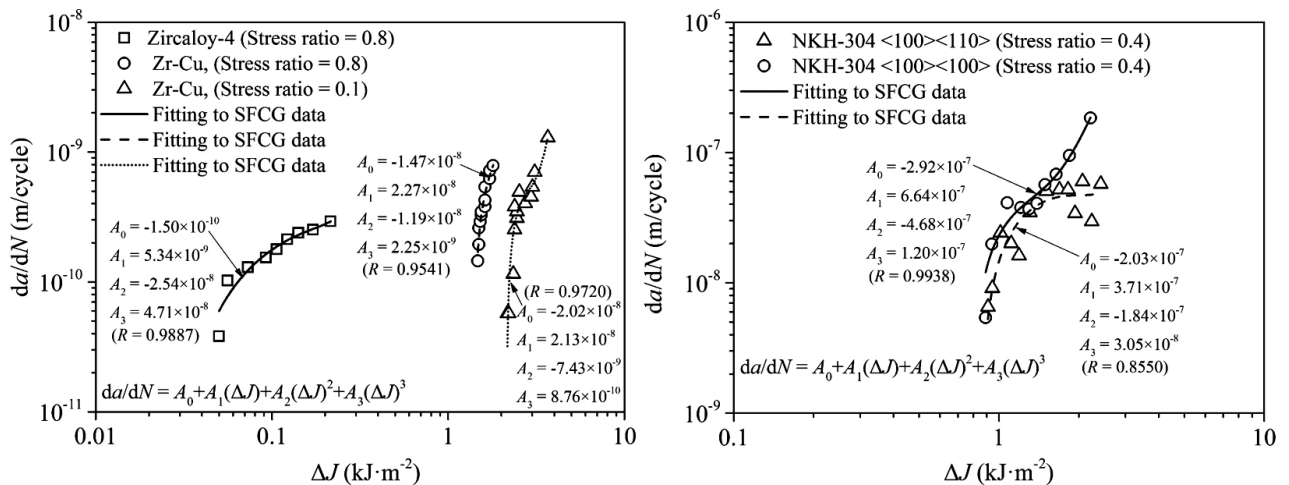


Figure 5: Curves of fatigue-crack growth rate versus ΔJ for Zr alloy¹³ and Ni-based single-crystal superalloy (NKH-304)^{14,15}

acteristic between them that needs to be expressed by high-order terms.

Besides, the proposed model has the ability to be used for a wide range of applications due to its high-order terms, which can be validated by various materials using experimental data from the literature, such as the Zr alloy and Ni-based single-crystal superalloy, as shown in **Figure 5**. The third-order nonlinear relationship can describe the behavior of SFCG.

4 CONCLUSIONS

In the paper, the *in-situ* fatigue-crack observation test is conducted to monitor and record the crack length in real time. The relationship between the fatigue crack's growth rate and ΔJ is determined by the formula based on the FE method and *in-situ* fatigue test data. The conclusions are as follows:

(1) The *in-situ* fatigue-crack observation platform consists of the fatigue test system and an optical measurement system. The micron-level fatigue cracks can be observed and recorded during the fatigue loading test. The effect of the artificial corrosion pit with a deflection angle on the fatigue crack growth path is proposed and studied. The results show that the fatigue crack growth deflection angle decreases with the increasing fatigue-crack length, which is affected by the symmetry of the specimen's geometry and the fatigue loading.

(2) The relationship between the parameters characterizing the nonlinear stress field at the front of short fatigue crack and the fatigue crack growth rate is established empirically. It is demonstrated that the SFCG rate of 35CrMo steel is in the range $(0.3\text{--}1.5)\times 10^{-3}$ mm/cycle. The abrupt change of the slope of da/dN versus ΔJ means that the growth rate increases first and then decreases with the short fatigue crack growth. The critical value of ΔJ of the short fatigue crack is in the range $3.7\text{--}6.2$ kJ/m², which is the main reason for the nonlinear relationship between the SFCG rate and the J -integral. Furthermore, the relationship exhibits good flexibility for modelling the SFCG behaviour of metals, which provides a quantitative relationship model for fatigue failure research of metals and alloys.

Acknowledgment

The authors acknowledge the National Key R&D Program of China (No. 2023YFB3709904), Special Project for Industrial Infrastructure Reconstruction & High

Quality Development of Manufacturing Industry (2023ZY01074) for funding.

5 REFERENCES

1. J. Ricardo Tarpani, D. Spinelli, Linear elastic vs elastic-plastic fracture mechanics methods in nuclear vessel integrity assessments, *Int. J. Pres. Ves. & Piping*, 74 (1997) 2, 97–103, doi:10.1016/S0308-0161(97)00076-8
2. S. T. Lie, T. Li, Failure pressure prediction of a cracked compressed natural gas (CNG) cylinder using failure assessment diagram, *J. Nat. Gas Sci. Eng.*, 18 (2014), 474–483, doi:10.1016/j.jngse.2014.03.021
3. J. Zhang, Z. Lian, Z. Zhou, Z. Song, M. Liu, K. Yang, Z. Liu, Safety and reliability assessment of external corrosion defects assessment of buried pipelines—soil interface: A mechanisms and FE study, *J. Loss Prevent. Proc.*, 82 (2023), 105006, doi:10.1016/j.jlp.2023.105006
4. P. Chen, X. Zha, L. Gao, X. Zhang, X. Liu, Modeling and Analysis on Surface Crack Propagation and Life Time Prediction of Gas Cylinder, *Dev. Appl. Mater.*, 32 (2017), 5–12, doi:10.19515/j.cnki.1003-1545.2017.05.002
5. Y. Pronina, O. Sedova, M. Grekov, T. Sergeeva, On corrosion of a thin-walled spherical vessel under pressure, *Int. J. Eng. Sci.*, 130 (2018), 115–128, doi:10.1016/j.ijengsci.2018.05.004
6. D. Kumar, K. K. S. Mer, H. S. Payal, K. Kumar, Residual stress modeling and analysis in AISI A2 steel processed by an electrical discharge machine, *Mater. Tehnol.*, 56 (2022) 1, 65–72, doi:10.17222/mit.2021.325
7. P. Paris, F. Erdogan, A Critical Analysis of Crack Propagation Laws, *J. Basic Eng.*, 55 (1963), 528–534, doi: 10.1115/1.3656900
8. J. Bulloch, Fatigue threshold in steels—Mean stress and microstructure influences, *Int. J. Pres. Ves. & Piping*, 58 (1994) 1, 103–127, doi:10.1016/0308-0161(94)90013-2
9. D. Kujawski, Estimations of stress intensity factors for small cracks at notches, *Fatigue Fract. Eng. M.*, 14 (1991), 953–965, doi:10.1111/j.1460-2695.1991.tb00005.x
10. Q. Sun, Q. Liu, X. Li, Z. Cai, X. Huo, M. Fan, Y. He, X. Yao, J. Pan, K. Li, Near-threshold fatigue crack growth behavior of the weld metal and heat-affected zone in an ex-service CrMoV steel joint, *Int. J. Fatigue*, 164 (2022), 107175, doi:10.1016/j.ijfatigue.2022.107175
11. J. Bulloch, Near threshold fatigue crack propagation behaviour of CrMoV turbine steel, *Theoret. Appl. Fract. Mech.*, 23 (1995) 1, 89–101, doi:10.1016/0167-8442(95)00007-2
12. J. Hou, J. Lv, A. Ricoeur, Y. Hu, H. Zuo, Y. Chen, Q. Li, The M-integral in fracture and damage mechanics: A review of developments and applications, *Eng. Fract. Mech.*, 273 (2022), 108741, doi:10.1016/j.engfracmech.2022.108741
13. M. Sakaguchi, R. Komamura, X. Chen, M. Higaki, H. Inoue, Crystal plasticity assessment of crystallographic Stage I crack propagation in a Ni-based single crystal superalloy, *Int. J. Fatigue*, 123 (2019), 10–21, doi: 10.1016/j.ijfatigue.2019.02.003
14. S. Wisner, M. Reynolds, R. Adamson, Fatigue behaviour of irradiated and unirradiated Zircaloy and Zirconium, In: Tenth international symposium on zirconium in the nuclear industry, 1993, 499–520
15. W. Logsdon, P. Liaw, Tensile, fracture toughness, and fatigue crack growth rate properties of zirconium copper, In: Springer-Verlag New York Inc., 1987